Neuron
Article

A Radial Glia-Specific Role of RhoA in Double Cortex Formation

Silvia Cappello,[1,9] Christian R.J. Böhringer,[1,9] Matteo Bergami,[2] Karl-Klaus Conzelmann,[3] Alexander Ghanem,[3] Giulio Srubek Tomassy,[4] Paola Arlotta,[4] Marco Mainardi,[5] Manuela Allegra,[5] Matteo Caleo,[5] Jolanda van Hengel,[6,7] Cord Brakebusch,[8] and Magdalena Götz[1,2,*]

[1]Helmholtz Center Munich, German Research Center for Environmental Health, Institute for Stem Cell Research, 85764 Neuherberg, Germany
[2]Physiological Genomics, University of Munich, 80336 Munich, Germany
[3]Max von Pettenkofer Institute and Gene Center, University of Munich, 80336 Munich, Germany
[4]Department of Stem Cell and Regenerative Biology, Harvard University, Cambridge, MA 02138, USA
[5]CNR Neuroscience Institute, 56100 Pisa, Italy
[6]Department of Molecular Biomedical Research, VIB, Ghent University, Ghent 9052, Belgium
[7]Department of Biomedical Molecular Biology, Ghent University, Ghent 9052, Belgium
[8]Faculty of Health Sciences, Institute of Molecular Pathology, University of Copenhagen, 2200 Copenhagen, Denmark
[9]These authors contributed equally to this work
*Correspondence: magdalena.goetz@helmholtz-muenchen.de
DOI 10.1016/j.neuron.2011.12.030

SUMMARY

The positioning of neurons in the cerebral cortex is of crucial importance for its function as highlighted by the severe consequences of migrational disorders in patients. Here we show that genetic deletion of the small GTPase RhoA in the developing cerebral cortex results in two migrational disorders: subcortical band heterotopia (SBH), a heterotopic cortex underlying the normotopic cortex, and cobblestone lissencephaly, in which neurons protrude beyond layer I at the pial surface of the brain. Surprisingly, *RhoA*$^{-/-}$ neurons migrated normally when transplanted into wild-type cerebral cortex, whereas the converse was not the case. Alterations in the radial glia scaffold are demonstrated to cause these migrational defects through destabilization of both the actin and the microtubules cytoskeleton. These data not only demonstrate that RhoA is largely dispensable for migration in neurons but also showed that defects in radial glial cells, rather than neurons, can be sufficient to produce SBH.

INTRODUCTION

A hallmark of the mammalian neocortex is the arrangement of functionally distinct neurons in six horizontal layers, which possess distinct properties in different sensory or motor areas (Leone et al., 2008; Molyneaux et al., 2007). The importance of this arrangement is revealed when it is disturbed, such as in patients with brain malformations, which are largely composed of neuronal dysplasia in the cerebral cortex (Bielas et al., 2004; Guerrini and Parrini, 2010; Ross and Walsh, 2001). One group of malformations, periventricular heterotopia (PH), results in cortical gray matter (GM) of varying size located at the ventricular margin. These defects can be associated with epilepsy and mental retardation (Guerrini and Parrini, 2010). While PH is clinically heterogeneous and also exhibits locus heterogeneity, most of the X-linked cases are due to mutations in a gene encoding the F-actin binding phosphoprotein Filamin A (Guerrini and Parrini, 2010; Robertson, 2004). A second group of neuronal migration disorders consists of mutations in genes encoding microtubule (MT)-associated proteins, like Doublecortin (DCX) and Lissencephaly-1 (LIS1), resulting in partial or incomplete migration of neurons to their cortical locations during development (Bielas et al., 2004; Ross and Walsh, 2001). Mutations at these loci can result in a "double cortex," a malformation which is distinct from PH in that the heterotopic GM is interposed between zones of white matter (WM), resulting in so-called subcortical band heterotopia (SBH). However, genetic inactivations of the murine homologs of genes mutated in human neuronal migration disorders so far have failed to reproduce these malformations, prompting the suggestion that mutations at other as-yet-unrecognized loci may result in SBH (Bilasy et al., 2009; Croquelois et al., 2009; Lee et al., 1997). These discrepancies highlight the complexity of human cerebral cortex in comparison to rodents. Not only do migrating neurons have to cover a much longer distance to their final destination, they also need to change radial guides more often due to the increase in pial surface compared to the ventricular surface with additional radial glia (RG) in the outer SVZ (Fietz et al., 2010; Hansen et al., 2010; Reillo et al., 2010). Thus, migrating neurons in human cerebral cortex may require other pathways as they face additional challenges during their journey. Moreover, radial glial cells may need specific pathways, which are yet ill-understood in the mouse model. Indeed, so far only mutation of MEKK4 has been suggested to affect migrating neurons and radial glial cells, causing disruption of the ventricular surface and protrusions of neuronal ectopia into the ventricle (Sarkisian et al., 2006).

Here we set out to examine the role of the small GTPase RhoA for neuronal migration in the developing cerebral cortex, as RhoA had been suggested to play key roles in directed cell migration in various tissues and organs (Govek et al., 2005; Heasman and Ridley, 2008). By using pharmacological means

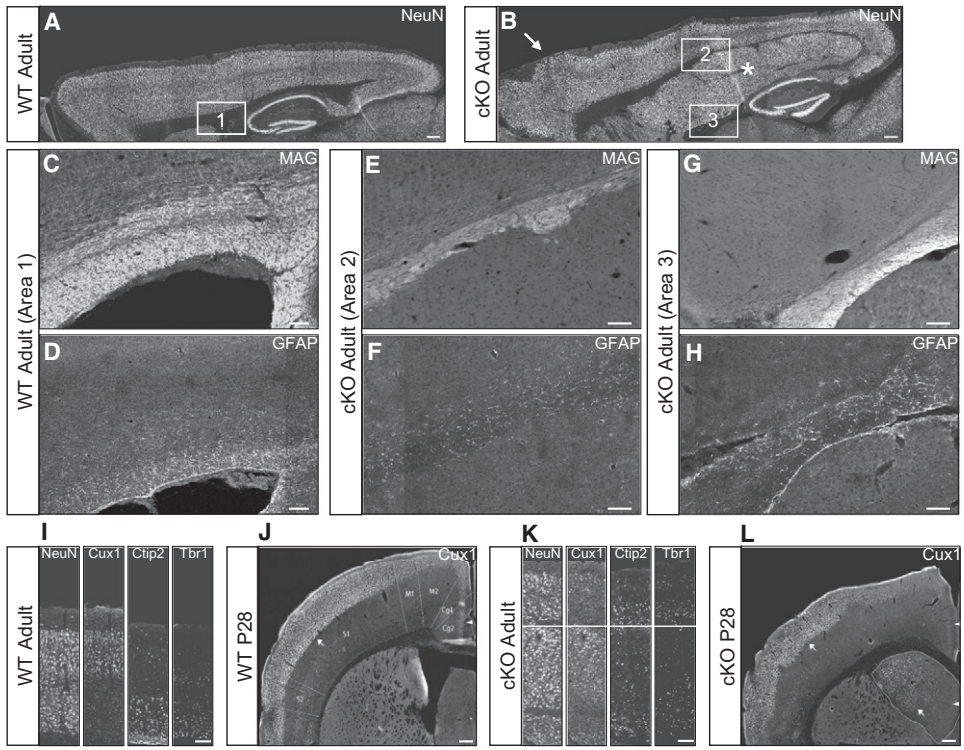

Figure 1. Characterization of SBH in cKO Adult Brains

(A–I and K) Micrographs of sagittal sections of the cerebral cortex from adult brains immunostained as indicated in the panels. Note in (B) the HC highlighted by the asterisk and the cobblestone-like structure pointed by the arrow.

(J and L) Micrographs of coronal sections of the cerebral cortex from P28 brains immunostained as indicated in the panels.

S1, primary somatosensory cortex; M1, primary motor cortex; M2, supplementary motor cortex; Cg1, cingulate cortex area 1; Cg2, cingulate cortex area 2. Scale bars: (A) and (B), 250 μm; (C)–(I) and (K), 100 μm; (J) and (L), 200 μm. See also Figures S1–S5.

and dominant-negative or constitutively active constructs, several studies suggested that RhoA is crucial for neuronal migration (Besson et al., 2004; Heng et al., 2008; Kholmanskikh et al., 2003; Nguyen et al., 2006; Pacary et al., 2011). However, the direct role of RhoA in neuronal migration has never been tested in the developing nervous system in vivo. Recently, conditional deletion of RhoA has revealed insights into its role at early stages of central nervous system (CNS) development in the spinal cord and midbrain, highlighting common functions in the maintenance of adherens junction coupling, as previously shown for other members of this family, such as Cdc42 and Rac1 (Cappello et al., 2006; Chen et al., 2009; Leone et al., 2010), but an opposite role in regulating cell proliferation in spinal cord versus midbrain (Herzog et al., 2011; Katayama et al., 2011). Moreover, neuronal migration or positioning of neurons was not examined in these mice at later embryonic or postnatal stages. We therefore set out here to delete RhoA in the brain region mostly affected by migrational disorders, namely, the cerebral cortex.

RESULTS

Deletion of RhoA in the Developing Cerebral Cortex Causes SBH

In order to determine the role of RhoA in neuronal migration during the development of the cerebral cortex, the Emx1::Cre mouse line driving recombination at early stages selectively in this region (Cappello et al., 2006; Iwasato et al., 2004) was crossed with mice containing exon3 of the RhoA gene flanked by loxP sites (Jackson et al., 2011). *Emx1::Cre/RhoA*$^{fl/fl}$ mice (henceforth referred to as cKO) were born at expected numbers, survived to adulthood, and exhibited no gross behavioral abnormalities. However, histological examination of their cerebral cortex revealed a striking phenotype, with a prominent tissue mass underneath an apparently layered but thinner cerebral cortex (Figures 1A and 1B; see Figure S1 available online). This heterotopic tissue was largely composed of NeuN^{+} neurons and exceeded the normotopic cortex (NC) in width within the occipital lobes (Figures 1A and 1B). To determine whether the heterotopic accumulation of neurons corresponds to the PH or SBH type, we stained for glial cells, as neurons are located directly at the ependymal lining of the ventricle in PH, while glial cells delineate neurons from the ventricle in SBH. Immunostaining for myelin proteins, such as myelin-associated glycoprotein (MAG; Figure 1C), labels the WM in WT cerebral cortex, and glia fibrillary acidic protein (GFAP) immunoreactivity also labels fibrous astrocytes within and subependymal astrocytes below the WM (Figure 1D). Interestingly, both GFAP and MAG label two horizontal bands in the cerebral cortex of cKO mice (Figures 1E–1H): an upper band below the NC but above the heterotopic cortex (HC; Figures 1E and 1F), which is also visible as a zone

free of neuronal nuclei (Figure 1B) and a lower horizontal band at the ventricle (Figures 1G and 1H). Thus, ectopic neurons are embedded within the WM and not directly apposed to the ventricle, defining this malformation as a form of SBH. In addition, NeuN$^+$ neuron clusters were also located in and even beyond the normally cell sparse layer 1 (Figure 1B, arrow, data not shown) at patches of basement membrane (BM) disruptions (Figures S7M and S7N), a migrational disorder referred to as type II cobblestone lissencephaly. Thus, conditional deletion of RhoA results in two migrational disorders.

In order to characterize the neuronal composition of the two cortices in the cKO mice, we first examined morphology and the polarity of neurons in the adult normotopic and heterotopic cortices. We performed in vivo injection of a spread-deficient G-pseudotyped rabies virus, in which the glycoprotein (G) was replaced by eGFP, in different layers of the adult WT and mutant cerebral cortex labeling individual neurons with a Golgi-like resolution. Analysis of neurons labeled in the upper normotopic cortex revealed a pyramidal neuron morphology with a dominant apically directed main dendrite reminiscent of normal pyramidal neurons (Figures S2A–S2D), as well as clearly distinct dendrites and a single axon (Figures S2A′–S2D′). Notably, we could trace some axons toward the callosum consistent with a correct morphological development of the respective labeled neurons and of their axonal projections (data not shown). Likewise, neurons in the SBH also exhibited clear axon-dendrite polarity, and some also had a pyramidal-like morphology, often inverted with the apical dendrite oriented toward the ventricle (Figures S2E–S2F′). We could also observe projections of neurons present in the SBH within both the upper and lower white matter (data not shown), suggesting that neurons in the NC and HC develop a grossly normal dendrite-axon polarity.

Neuronal subtypes in the cerebral cortex differ in regard to their layer and area position. We therefore first examined the laminar identity of the heterotopic neurons by immunodetection of sub-type-specific transcription factors, Cux1 for layers II/III and IV, Satb2 for layers II/III and V, Ctip2 and *Fezf2* for layers V and VI, and Tbr1 and Tle4 for layer VI. Neurons expressing these markers were arranged in the normal layered pattern in the NC in both WT and cKO mice. Interestingly, all of these markers were also observed in the SBH (Figures 1I–1L; Figure S3). However, most neurons in the HC/SBH were Cux1$^+$, indicating a primarily upper-layer identity, while the number of Cux1$^+$ neurons within the NC accordingly reduced (Figures 1K, 1L, and S3A). Interestingly, neurons expressing deep-layer markers (*Fezf2*, Ctip2, and Tle4) were often at the periphery of the SBH, while Cux1$^+$ and Satb2$^+$ neurons were localized in the core (Figures S3B–3SL), suggesting a concentric organization of neurons of different identities in the SBH by postnatal day (P)8 (Figures S3B–S3G). This organization was further confirmed by immunolabelling of the thalamo-cortical synapses positive for the vesicular glutamate transporter 2 (vGluT-2; Coleman et al., 2010; Figure S5C), revealing a series of blobs and stripes in the SBH of cKO mice (Figure S5C) supporting its nonlaminar organization. Moreover, a main stripe supposedly corresponding to layer 4 receiving these afferent fibers was also visible in the cKO NC but shifted upwards. Thus, neurons of all layers were present with a bias toward upper-layer neurons in the HC organized in a ring-like structure.

Deep-layer neurons (Tbr1$^+$, Ctip2$^+$) are normally generated first, and upper-layer neurons (Cux1$^+$, Satb2$^+$) are generated later during development. To examine this sequence in the cKO cerebral cortex, the DNA base analog BrdU was injected at E12, E14, and E16, and the distribution of BrdU$^+$ cells was examined at P7. We found cells born at all three stages in both NC and HC, with earlier generated neurons located at deeper positions in the NC as in the WT (Figure S4). Only few neurons generated at early stages (E12; Figures S4A and S4B) were detected in the HC, where the largest population of neurons was born at E16 (Figures S4E and S4F). This is in accordance with the layer marker analysis and further supports the notion that the SBH is mainly formed by late-born neurons.

Projection neurons of the cerebral cortex differ also in regard to their location within different cortical areas dedicated to distinct information processing tasks. Interestingly, the medial (low) to lateral (high) gradient in Cux1, Mdga1, and Rorβ expression, indicative of arealization in WT cerebral cortex, was detectable in the cKO NC (Figures 1J and 1L), and the SBH showed higher expression levels in the lateral and weaker at medial positions (Figures 1J and 1L; Figures S3M–S3P), suggesting some degree of arealization in both NC and HC. To test arealization at the functional level in the double cortex of cKO mice, we examined the primary visual (V1) and somatosensory (S1) cortex by measuring immediate-early gene (IEG) expression triggered by light exposure for 1.5 hr under normal lighting conditions after 3 days of complete darkness. Immunostaining for the IEG products c-Fos and Egr-1 revealed a strong signal in visual cortex areas of WT animals, while expression of both genes was significantly lower in both the upper and lower cortex of cKO mice (Figures S5A and S5B). However, light-induced IEG expression was confined to visual cortical areas as no upregulation of c-Fos was detectable in the primary somatosensory (S1) cortex (Figure S5A). Thus, despite its severe disorganization, the cKO cortex still possesses functional arealization.

Lastly, we examined the number of GABAergic neurons in the NC and HC, as their number is crucial for maturation of intracortical neural networks and plasticity (Gandhi et al., 2008; Huang et al., 1999; Lodato et al., 2011), and their migration into the cerebral cortex may have been affected by these severe alterations. However, GABAergic GAD67-positive neurons were present in normal numbers in the SBH (Figure S5D) and only slightly reduced in the NC of the cKO mice compared to controls (Figure S5D), suggesting that migration of GABAergic neurons is largely normal, but their number is not entirely sufficient to cover the increased size of the cKO cerebral cortex (1.32×, N = 4, p = 0.0001), intriguingly largely affecting the NC rather than the HC. Taken together, despite the profound alteration of a double cortex formation, neuronal subtype composition appears relatively normal.

Progenitor Proliferation in the cKO Cerebral Cortex

In order to understand when and how the prominent SBH is formed in the cKO mice, we first examined when RhoA protein disappears. While RhoA immunoreactivity was present throughout the WT cerebral cortex at embryonic day (E)12, it

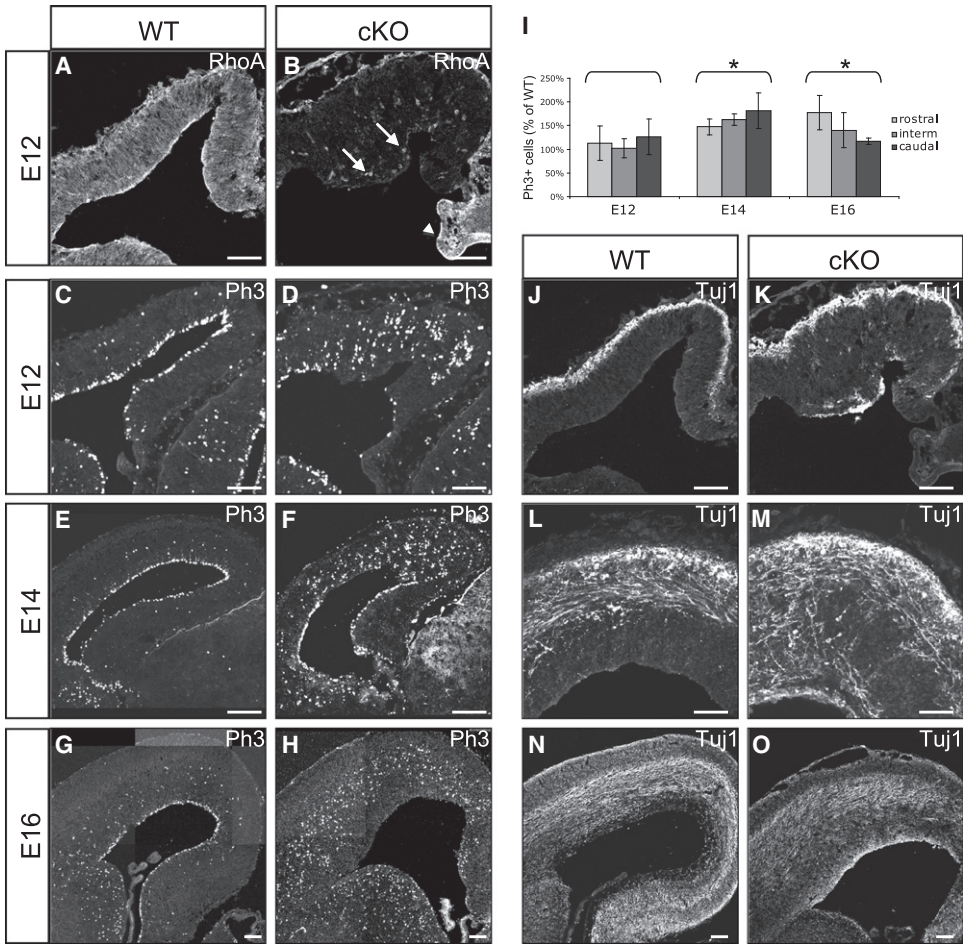

Figure 2. Proliferation and Differentiation in the RhoA cKO-Developing Cortex

(A–H and J–O) Micrographs of coronal sections of the cerebral cortex immunostained as indicated in the panels.

(I) Histogram showing the quantification of Ph3-positive cells.

Unequal variance t test, $p < 0.009$. Scale bars: (A)–(F), (J), and (K), 100 μm; (G), (H), and (L)–(O), 50 μm.

was largely absent in the cKO mice at this time (Figures 2A and 2B) but not yet at E11 (data not shown). As observed before (Cappello et al., 2006; Iwasato et al., 2004), Emx1::Cre-mediated recombination occurs specifically in the cerebral cortex, such that RhoA was still present in the neighboring plexus choroideus (Figure 2B, arrowhead) or the ganglionic eminence (GE, data not shown). Moreover, blood vessels depicted by arrows in Figure 2B also maintained RhoA, as Cre is not expressed in these cells. Already at E12, the first day of complete loss of RhoA protein in cKO mice, we noted a phenotype with mitotic cells stained for the phosphorylated form of histone 3 (Ph3) scattered in the cKO cerebral cortex in contrast to their alignment at the ventricular surface with few cells dividing at more basal positions in the cerebral cortex of control littermates (Figures 2C and 2D; see Experimental Procedures for terminology). Indeed, scattering of apical progenitors has also been observed when RhoA was deleted by other Cre lines in the midbrain or spinal cord (Herzog et al., 2011; Katayama et al., 2011). Given the increased thickness of the adult mutant cerebral cortex of about 1.3-fold, compared to the control mentioned previously, and effects on proliferation upon RhoA deletion in the spinal cord and midbrain, we also analyzed the number of $Ph3^+$ cells during development of the cerebral cortex. Notably, we observed a transient increase in the total number of Ph3-positive cells compared to WT littermates starting at occipital regions at E14 and later at E16 in rostral parts (Figures 2C and 2I), a pronounced difference to the profound reduction of proliferation after deletion of RhoA in the spinal cord. Thus, RhoA deletion affects proliferation in a region-specific manner within the cerebral cortex and differentially in distinct regions of the CNS (Herzog et al., 2011; Katayama et al., 2011).

Formation of a Proliferative Zone in the cKO Cerebral Cortex

In order to examine the etiology of the double cortex formation, we next examined progenitor and neuron localization at different time points. In accordance with the aberrant location of progenitor cells already at E12, some neurons labeled for βIII tubulin (Tuj1) were found in ectopic positions at the apical surface already at E12 (Figures 2J and 2K). Two days later, scattered progenitor cells had further spread covering the lower half of

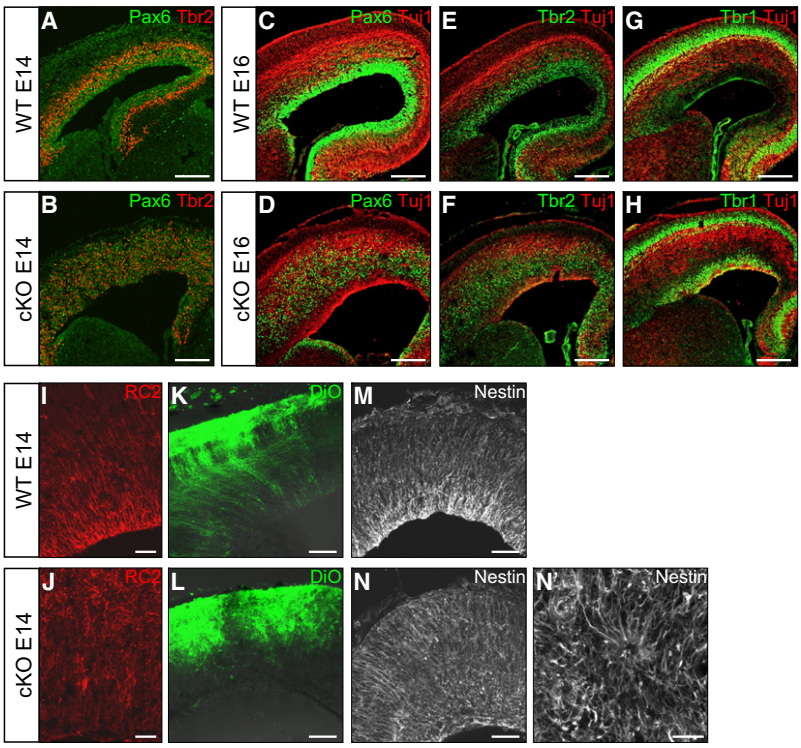

Figure 3. Characterization of Precursor Identity and Morphology in cKO-Developing Brains

(A–N′) Micrographs of coronal sections of the cerebral cortex immunostained as indicated in the panels. Note in panel (N′) the rosette-like structure.

Scale bars: (A)–(H), 100 μm; (I)–(N), 50 μm; (N′), 20 μm.

the cerebral cortex, and an increasing number of neurons were found mislocalized apically at the ventricular side (E14; Figures 2E, 2F, 2L, and 2M). Strikingly, by E16, mitotic cells had eventually assembled into a broad band located in the middle of the cerebral cortex between the pial and ventricular surfaces (Figures 2G and 2H). Interestingly, also the neurons had sorted out into two bands at this stage with an upper band corresponding to the cortical plate and a lower band of neurons located at the ventricular side below the progenitor zone (Figure 2N and 2O). The aberrant location of progenitors prompted the question of their identity and fate. Apical progenitors are RG expressing the transcription factor Pax6, while basally dividing cells express Tbr2 (Figure 3A; Englund et al., 2005). Despite their mispositioning, many progenitors were Pax6 or Tbr2 immunoreactive in the cKO cerebral cortex, with very few double-positive cells, as is the case in the cerebral cortex of control mice (Figure 3B). Indeed, also at latter stages when progenitors arrange in a band within the cerebral cortex, separate populations maintain Pax6 or Tbr2-expression respectively (Figures 3C–3F) and are framed on both sides by Tbr1-immuno-positive neurons (Figures 3G and 3H). Thus, by E16, when most of the upper-layer neurons are generated, the later organization of the double cortex has emerged with a slightly thinner (compared to WT) cortical plate at the basal side, supposedly generating the NC, and an ectopic neuron band, supposedly generating the HC at the apical side.

Disruption of the Radial Glial Scaffold in the cKO Cerebral Cortex

To determine to which extent the scattered Pax6$^+$ cells maintain their RG identity and to examine their characteristic radial morphology, we next stained for nestin and RC2 to reveal the radial glial processes (Figures 3I, 3J, 3M, and 3N). This also revealed scattered cell somata and rather disorganized processes, which were no longer aligned and radially oriented in the cKO cerebral cortex (Figures 3N and 3N′) in contrast to controls (Figure 3M). The loss of apical anchoring of radial glial cells (see above as indicated by the scattered Pax6$^+$ cells and below for F-actin analysis) further contributed to the disorganized arrangement of radial glia cell somata and processes. Indeed, many cells located apically had lost their adherens junction anchoring (Figure S7) but were still able to form points of adhesion as also visible in rosette-like structures sometimes observed between nestin$^+$ cells in the cKO cerebral cortices with processes emanating radially and in rare cases directed to the pial or ventricular surface (Figure 3N′). As it appeared from these stainings that RG processes do no span the radial thickness of the cKO cerebral cortex, we examined this more globally by applying the lipophilic tracer DiO onto the surface of the cortices. As described previously (Malatesta et al., 2000), this label spreads along RG processes to their somata located in the ventricular zone (VZ; Figure 3K). In the cKO cortices, however, DiO-labeled processes were arranged in a very disorganized manner, and only few labeled processes reached the VZ (Figure 3L). Interestingly, the bulk of the DiO-labeled processes ended in the middle of the cerebral cortex, consistent with the idea that the upper and lower halves of the cKO cerebral cortex are no longer connected by radial processes.

The Effect of RhoA in Migrating Neurons

The above data suggest that aberrations in radial glial cells, the main guides for migrating pyramidal neurons, may be responsible for the failure of many neurons to reach their normal position. However, RhoA may also affect neuronal migration directly by affecting the cytoskeleton in migrating neurons as previously suggested (Besson et al., 2004; Heng et al., 2010; Nguyen et al., 2006). To test these possibilities, we first electroporated CreGFP or GFPonly plasmids into the cerebral cortex of E14 *RhoA*$^{fl/fl}$ embryos to delete RhoA in few cells and examined RhoA levels 1 day later (Figure S6). Consistent with the fast reduction of RhoA protein, we observed a notable reduction of RhoA-immuno-reactivity in the electroporated regions compared to neighboring parts, where no electroporated cells were located (Figures S6A–S6C). CreGFP-electroporated cells distributed along the entire cortex 3 days later (Figures 4A

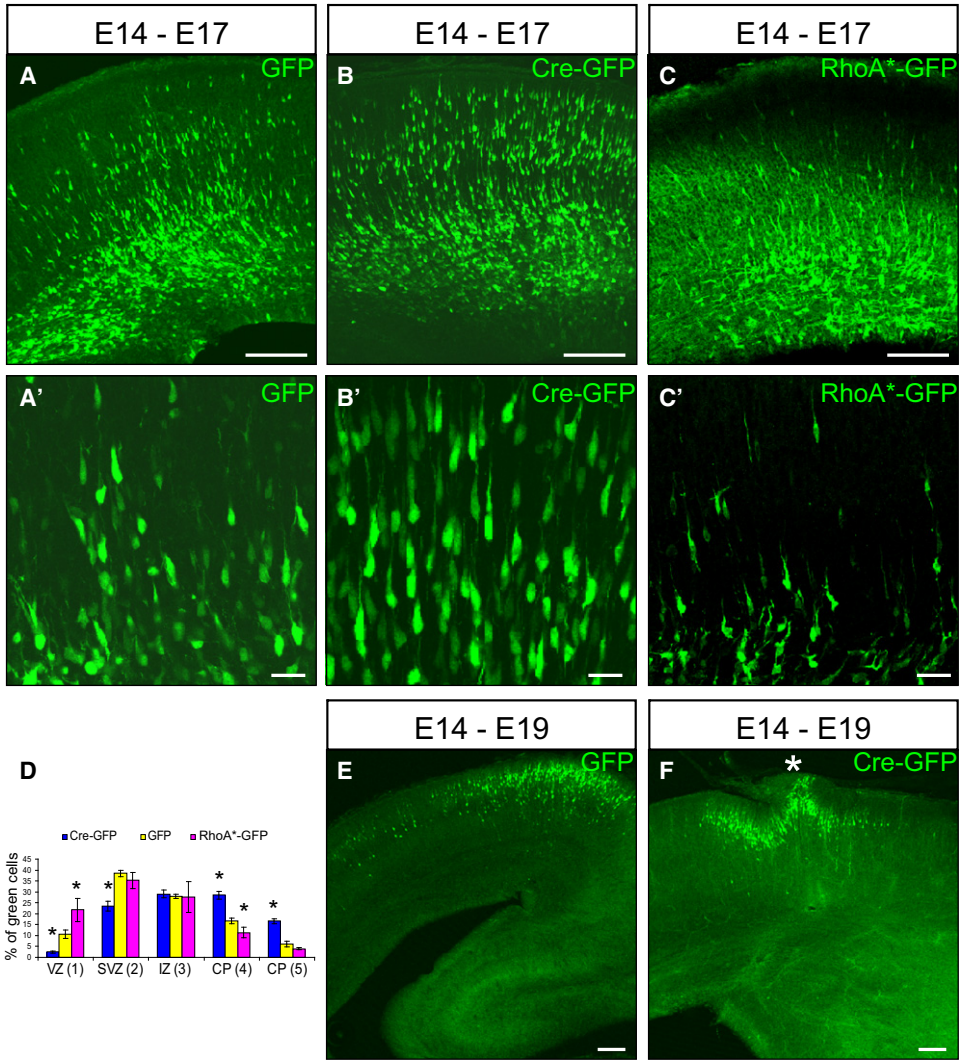

Figure 4. Normal Migration of cKO Cells in Developing Brains

(A and C′) Micrographs of coronal sections of the cerebral cortex electroporated at E14 and analyzed at E17.

(D) Histogram showing the distribution of GFP- versus Cre-GFP- and RhoA*-GFP-transfected cells 3 days after electroporation. The cortex was subdivided into five equally thick bins approximately corresponding to VZ (bin 1), SVZ (bin 2), IZ (bin 3), and CP (bins 4 and 5).

(E and F) Micrographs of coronal sections of the cerebral cortex electroporated at E14 and analyzed at E19.

Student's t test, $p < 0.005$ for bins 1, 2, 4, and 5 (Cre-GFP) and for bins 1 and 4 (RhoA*-GFP); N = 3 per genotype.

CP, cortical plate; IZ, intermediate zone; SVZ, subventricular zone; VZ, ventricular zone. Scale bars: (A–C), (E), and (F), 100 μm; (A′), (B′), and (C′), 20 μm. See also Figure S6.

and 4B), with many neurons with apparently normal morphology in the cortical plate (Figures 4A′ and 4B′). Quantification of the proportion of GFP-labeled cells (CreGFP-electroporated cells in *RhoA*$^{fl/+}$ animals or GFP-electroporated cells in *RhoA*$^{fl/fl}$ embryos were used as a control; Figure 4D, yellow bars) confirmed not only the efficient neuronal migration but even revealed an apparently faster migration of RhoA-depleted neurons as a significantly higher proportion of GFP$^+$ cells was located in the upper most bin of five equally bins, corresponding to the cortical plate (CP), compared to controls (Figure 4D, blue bars). These experiments therefore suggest that RhoA-depleted neurons did not fail to migrate but rather migrated faster than control cells. Some RhoA-depleted cells had migrated even beyond the CP forming ectopic clusters within and beyond layer 1 in brains analyzed at E19, i.e., 5 days after electroporation (Figures 4E and 4F), reminiscent of the type II cobblestone lissencephaly observed in the cerebral cortex of cKO mice and described previously. To test the possibility that RhoA may indeed slow down migration and release this break in its absence, we electroporated a spontaneously activated ("fast-cycling") mutant of RhoA (RhoA*) and quantified the position of GFP$^+$ cells in the cerebral cortex. Indeed, consistent with this scenario, we detected a significant increase of GFP-labeled cells in the lower layers 3 days after

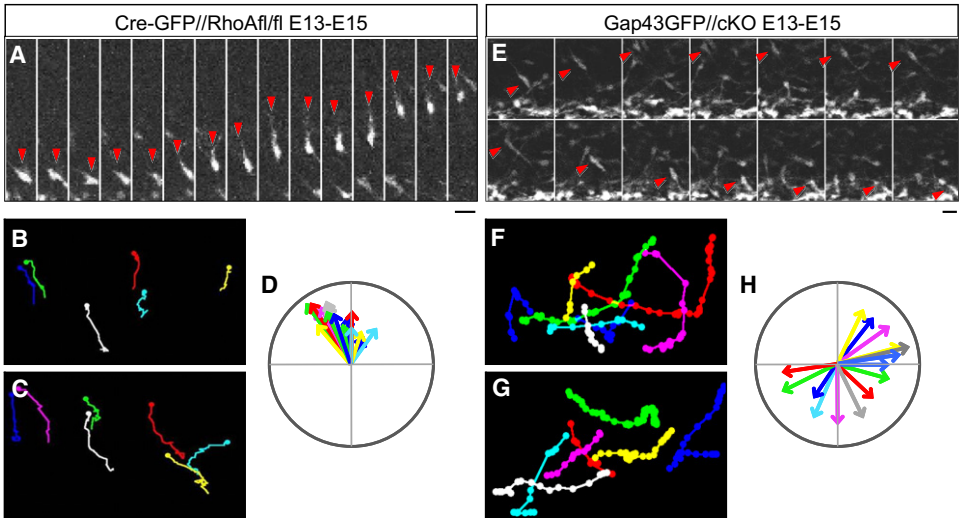

Figure 5. Time-Lapse Imaging of RhoA-Deficient Migrating Neurons

(A and E) Micrographs of coronal slices of the cerebral cortex electroporated at E13 and analyzed at E15 as depicted in the panels.

(B and C) Traces of Cre-electroporated migrating cells 48 hr after electroporation analyzed for 9 hr at 10 min intervals (n = 3).

(F and G) Traces of Gap43GFP-electroporated cells 48 hr after electroporation analyzed for 12 hr at 10 min intervals (n = 2).

(D and H) Direction of migrating cells in (B and C) and (F and G), respectively, plotted with the pial surface up and the ventricular surface down. Note the largely radial migration of Cre-electroporated cells in WT environment, while cells in the lower cKO cortex migrate in many directions with no clear radial preference. Scale bars: 10 μm.

electroporating the fast-cycling RhoA mutant construct (Figures 4C, 4C′, and 4D, pink bars), suggesting a delay in migration in the condition of activated RhoA.

Even though these migrating neurons also had a normal polarized morphology, consistent with a normal migration, it would still be possible that RhoA-deficient neurons reach their final position but in a very different or disturbed migration compared to normal. We therefore directly monitored the migration of electroporated cells by live imaging in slices. E13 Cre-electroporated cortices were sliced and sections were imaged 2 days after transfection for approximately 9 hr to examine the movement of migrating cells (Movie S1; Figures 5A–5D). All cells imaged performed a normal radial migration moving basally and directed by a single leading process, as shown by the traces of tracked cells in Figures 5A–5D.

However, despite the early reduction of RhoA protein in electroporated regions, the remnant levels may still be sufficient to allow for migration of these neurons. To examine migration of neurons lacking RhoA protein entirely, we employed transplantation experiments with cells from E14 cKO cortices which had completely lost RhoA protein by E12. E14 cells were dissociated and labeled with cell tracker green prior to transplantation into isochronic WT cortices (Figures 6A and 6B). Similar to control cells also *RhoA*$^{-/-}$ cells had often reached the IZ or CP 3 days after transplantation (Figures 6C–6E). Thus, neurons still migrate fairly normal and reach the CP also in the complete absence of RhoA.

WT Cells Transplanted in cKO Cerebral Cortex Contribute to Normo- and Heterotopic Cortices

The above observations do not support the hypothesis that a migration defect is the cause for SBH formation, as neurons devoid of RhoA can still migrate fairly normal. We therefore tested the effect of RhoA depletion in radial glial cells by examining how WT cells would behave in cKO brains and transplanted green-labeled cells from E14 WT into E14 cKO cerebral cortices. Notably, more cells integrated into the cKO cortices, probably due to the disrupted junctional coupling at the ventricular surface (see below). Interestingly, 3 days after transplantation, we observed transplanted WT cells either in the normotopic cortical plate (Figure 6F) or accumulating within the lower cortical regions without any spread toward the pial surface (Figure 6G). Thus, the distribution of WT cells within a cKO cortex mirrored the distribution of endogenous cells in an upper and a lower band. To directly visualize whether WT cells would contribute to the SBH, transplanted cKO mice were examined at P2, when the SBH was clearly visible and contained many of the transplanted WT cells (Figure 6H). These results therefore imply non-cell-autonomous effects for the formation of the double cortex.

To directly visualize the motility of RhoA-depleted cells in the disorganized radial glia scaffold in the mutant cortex, we performed live imaging of GFP-labeled cells in slices after electroporation of a membrane-tagged GFP (Gap43-GFP) into the cKO cerebral cortex at E13 (Movie S2). Two days after electroporation, we found many cells migrating. Intriguingly, however, migration was rarely radially oriented, and in most cases, migration was actually tangentially oriented (see Movie S2; Figures 5E–5H). Taken together, these data demonstrate that RhoA-depleted cells can migrate well but follow a largely nonradial path when the radial glia scaffold is disturbed.

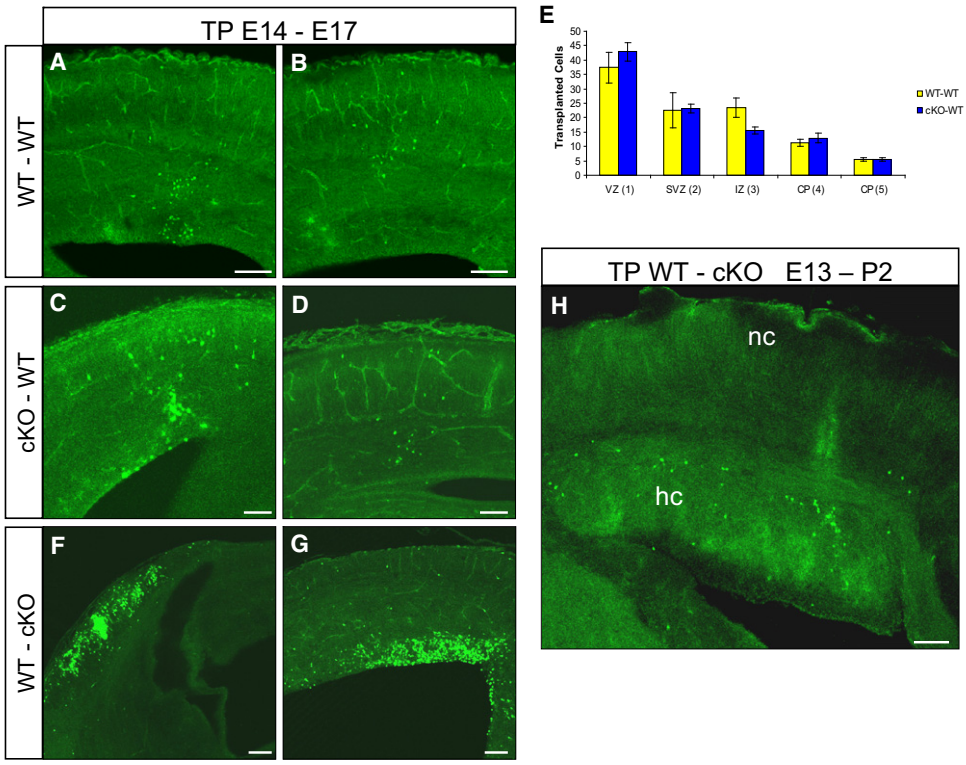

Figure 6. Impaired Migration of WT Cells in cKO Brains

(A–D, F, and G) Micrographs of coronal sections of the cerebral cortex transplanted with green-labeled cells at E14 and analyzed at E17.

(E) Histogram showing the distribution of WT cells transplanted into WT embryos compared to distribution of cKO cells transplanted into WT embryos 3 days after transplantation. The cortex was subdivided into five equally thick bins approximately corresponding to VZ (bin 1), SVZ (bin 2), IZ (bin 3), and CP (bins 4 and 5).

(H) Micrograph of a coronal section of the cerebral cortex transplanted at E13 and analyzed at P2.

n = 3 per genotype.

Scale bars: 100 μm.

RhoA Affects the RG Scaffold Most Severely by Alterations in Both the Actin and Microtubules Cytoskeleton

Given the importance of the scaffold aberration suggested by the above experiments, we next asked how the absence of RhoA signaling may affect RG organization and how these effects may differ in neurons.

First, we examined the actin cytoskeleton, since actin polymerization into fibers (F-actin) is a well-established function of RhoA (Etienne-Manneville and Hall, 2002). Indeed, when cells from E14 WT and cKO cerebral cortex labeled for F-actin by phalloidin were analyzed one day after plating in vitro, actin fibers were clearly less in the cKO cells (Figures 7A and 7B). To determine whether conversely the globular form of actin is increased and to which extent this is the case in vivo, we separated F-actin from G-actin by ultracentrifugation and immunoblotted the fractions obtained from E14 WT and cKO cerebral cortices (Figure 7C). Indeed, the G-actin signal was increased by 30% in the cKO compared to WT cortex (Figure 7D), suggesting a shift in the F- to G-actin ratio in cells lacking RhoA.

One of the main sensors of the F- to G-actin ratio is MAL, a cofactor of SRF (Vartiainen et al., 2007). MAL bound to G-actin in the cytoplasm cannot translocate to the nucleus to promote SRF-mediated transcription, but upon actin polymerization, e.g., by RhoA activation, monomers of actin are converted into fibers and MAL is released and translocates into the nucleus (Connelly et al., 2010). We therefore examined the cytoplasmic and nuclear levels of MAL in E14 WT and cKO cerebral cortex and observed a prominent increase in the cytoplasmic MAL levels (Figures 7E and 7F), consistent with the concept that increased levels of actin monomers retain MAL in the cytoplasm.

A further readout of alterations in the F-actin formation are junctional complexes between epithelial cells, as connecting rings of actin fibers are crucial for the stabilization of epithelial cell-cell junctions (Vasioukhin and Fuchs, 2001). If their formation were compromised, this should result in cell scattering and disassembly at the apical surface as observed in other mutants with defects in junctional coupling (Cappello et al., 2006; Lien et al., 2006; Machon et al., 2003). Indeed, immunostaining for β-catenin, pan-cadherin, and Par3 revealed large patches of ventricular surface devoid of junctional and apical bands in the E12 cKO cerebral cortex but not the adjacent GE (Figure S7A–S7H″). Similarly, examination of junctional complexes at the ultrastructural level readily revealed electrondense junctional complexes in the WT E13 VZ, while few such complexes

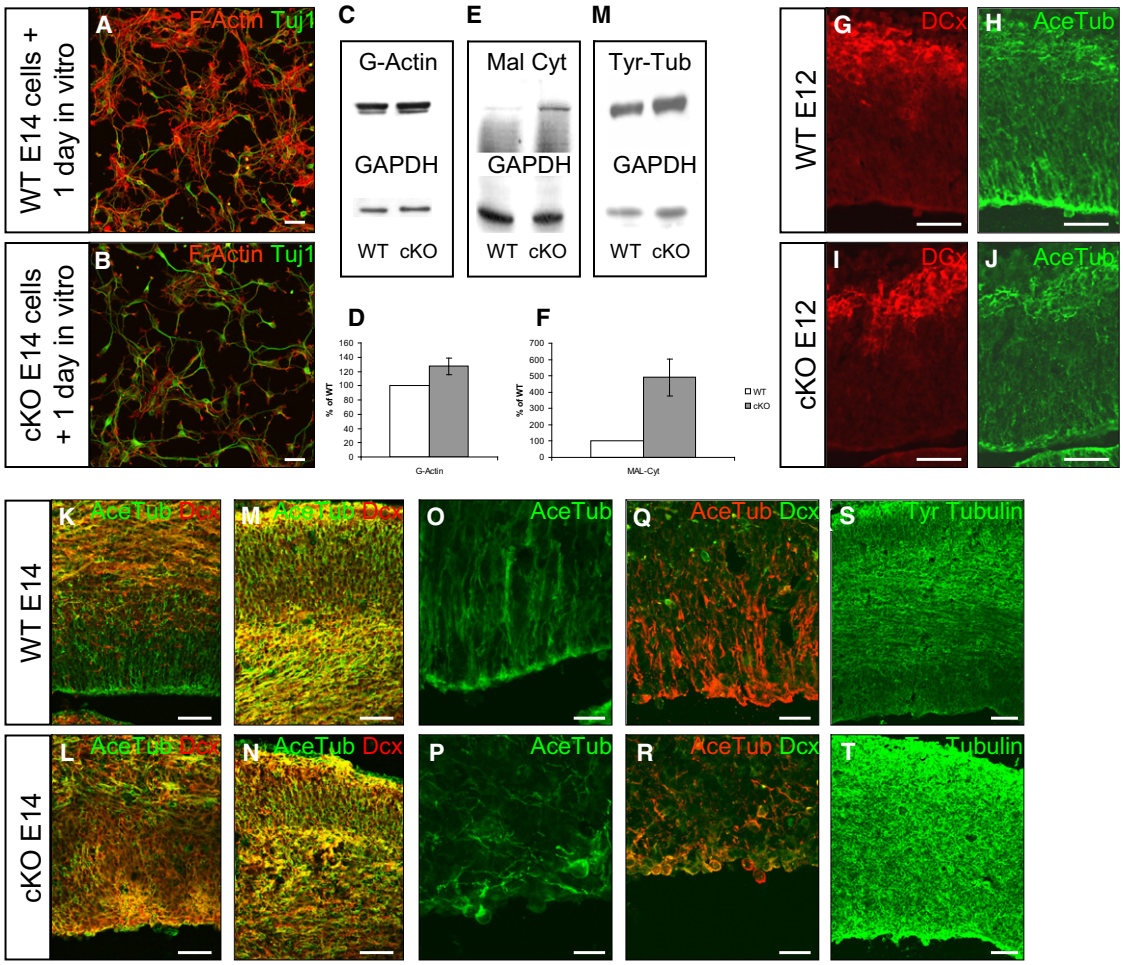

Figure 7. Actin Polymerization and Microtubules Stability Is Impaired in Mutant Brains

(A and B) Cortical cultures from E14 brains immunostained as indicated in the panels.

(C, E, and M) Western blot of cortical tissue from E14 brains.

(D and F) Histogram showing the quantification of the normalized signals obtained from (C) and (E), respectively.

(G–T) Micrographs of coronal sections of the cerebral cortex immunostained as indicated in the panels.

Student's t test, $p < 0.03$; $n = 3$.

Scale bars: (A), (B), (G–N), (S), and (T), 50 μm; (O)–(R), 20 μm. See also Figure S7.

were visible at the ventricular surface in the cKO cerebral cortex (Figures S7I and S7J), confirming the absence of junctional anchoring at the apical surface in the absence of RhoA. However, points of adhesion that could still be formed as junctional complexes were present in the rosette-like structures (Figure S7J′), where they are less exposed to strong forces as at the apical surface of the growing telencephalon. Indeed, the enrichment of AJs at the apical surface, as monitored by the β-catenin$^+$ apical band, was missing at E14 in the mutant cortex (Figures S7K and S7L). Thus, while loss of RhoA destabilized the actin cytoskeleton in both neurons and radial glial cells, it has most severe consequences on the radial glia scaffold abolishing its apical anchoring.

Moreover, deletion of RhoA also resulted in destabilization of microtubules (MTs) mostly in radial glial cells but less so in neurons. Indeed, RhoA signaling has previously been described to stabilize MTs in nonneuronal cells (Etienne-Manneville and Hall, 2002), and accordingly immunoreactivity for dynamic tyrosinated MTs was much higher in the cKO than WT cortex (Figures 7S and 7T), as also confirmed by western blot (Figure 7M). Conversely, immunostaining for stable, acetylated MTs labeled RG processes in WT (Figures 7G and 7H), while RGs in the cKO cortex had already weaker levels of immunoreactivity at E12 (Figures 7I and 7J) and virtually lost any labeling for acetylated tubulin by E14 (Figures 7O and 7P). Most strikingly, however, the remaining acetylated tubulin staining localized almost exclusively to neuronal processes present at ectopic positions in the VZ (Figure 7K–7N and 7Q–7R). Thus, in addition to destabilizing the actin cytoskeleton, loss of RhoA also severely destabilized microtubule in radial glia but less so in neurons. The combined effects on the actin and microtubule cytoskeleton promoting disassembly of the actin filaments and

the turnover of MTs thus causes the severe defects of the radial process arrangement of radial glial cells and thereby abrogate the stabile scaffold for migrating neurons.

DISCUSSION

This analysis of RhoA function in the developing cerebral cortex revealed several surprising results in regard to the phenotype observed, the formation of a prominent double cortex or SBH, as well as in regard to the lack of phenotypes observed, such as the relatively normal migration and process formation of neurons lacking RhoA. Whereas RhoA was apparently largely dispensable in neurons, the lack of RhoA resulted in profound defects in RG with defects in adherens junction coupling and apical anchoring, as well as defects in process formation or maintenance. Most importantly, this cell-type-specific function of RhoA now sheds light on the etiology of the ''double cortex'' malformation by affecting the migration scaffold rather than the migrating neurons themselves.

Role of RhoA in Migrating Neurons

The rather ubiquitous small RhoGTPases have been involved in many functions, including the formation of process asymmetry and the initiation and maintenance of migration in cortical neurons (Ge et al., 2006; Hand et al., 2005), but much of these insights have been gained by using constitutively active and dominant-negative constructs in vitro (Hall and Lalli, 2010). The selective deletion of individual small GTPases in vivo now allows examining their role in vivo in a region and cell-type-specific manner. Consistent with our analysis in the forebrain, RhoA deletion results also in the midbrain and spinal cord in scattering of progenitors and neurons and loss of stable adherence junction coupling (see below; Herzog et al., 2011; Katayama et al., 2011). While the overall phenotype of scattered neurons—resulting only in the cerebral cortex in the prominent SBH—may have been interpreted as RhoA playing a role at least also in migrating neurons, our work shows by transplantation, live imaging, and Cre-electroporation experiments that the lack of RhoA does not interfere with the initiation or continuation of migration or with process formation, maintenance, or nucleokinesis in neurons. In a WT environment, RhoA cKO neurons could initiate migration and reach the cortical plate within a few days with an apparently normal morphology, including a prominent apical dendrite. This was shown by Cre electroporation, as well as by transplantation of cells lacking RhoA entirely, as they were derived from the Emx1::Cre-mediated deletion several days after onset of recombination. It is worth noting that RhoA protein decreased within 24 hr of Cre electroporation at E14 and was completely gone 2 days after onset of Emx1::Cre-mediated recombination in early progenitors (E10) of the cerebral cortex, while it is remarkably stable in postmitotic neurons. This is why it is not possible to delete RhoA in neurons sparing radial glial cells, as RhoA protein was still detected at E16 in neurons of the cerebral cortex in Nex-Cre (Goebbels et al., 2006) or Ngn2-Cre (Berger et al., 2004) $RhoA^{fl/fl}$ mice, where largely basal progenitors are targeted (data not shown). However, the transplantation experiments unequivocally show that neurons deficient of any detectable RhoA protein levels migrate well toward the cortical plate.

These data are consistent with the concept that Rac1 and Cdc42 are responsible for the formation of the leading process (Wheeler and Ridley, 2004) and that overactivation of RhoA stalls migration of neurons. Indeed, we show here that electroporation of the fast-cycling form of RhoA resulted in slower neuronal migration, while neurons with reduced levels of RhoA upon Cre electroporation reached the cortical plate faster. Consistent with this concept, $RhoA^{-/-}$ neurons showed a clear decrease in F-actin formation and also migrated faster in dissociated cell cultures (Figure S6H) and in vivo (Figure 4D). These data are well consistent with previous work rescuing delayed neuronal migration by inactivation of RhoA or inhibition of ROCK, a direct target of RhoA (Hand et al., 2005; Kholmanskikh et al., 2003; Pacary et al., 2011). Likewise, gelsolin, an F-actin severing protein, is important for migration of adult-generated neurons (Kronenberg et al., 2010), while deletion of RhoA in adult neurogenesis did also not impair the migration of neuroblasts to the olfactory bulb (data not shown). Thus, RhoA slows down migrating neurons via stabilizing the actin cytoskeleton and F-actin formation, but the level of F-actin regulation mediated by RhoA appears to play a relatively minor role in neurons of the developing cerebral cortex.

This is surprising given that the balance between F- and G-actin regulates the orientation of neuronal migration in the developing cerebral cortex (Pinheiro et al., 2011). Interestingly knock-down of Lpd results, via increase of G-actin levels and inhibition of SRF-mediated transcription, in a preferential tangential migration of neurons. However, loss of RhoA also results in increased levels of G-actin, but—at least in a WT environment—$RhoA^{-/-}$ neurons still manage to migrate radially suggesting that the G-actin levels are not yet sufficiently high to mediate the switch to a tangential mode of migration. Thus, other mechanisms besides RhoA contribute to achieve sufficiently high levels of F-actin and low levels of G-actin. It is important to note that several signaling pathways, mediated by ECM components of the basement membrane or the secreted signaling molecule reelin promote phosphorylation of cofilin and thereby F-actin formation and maintenance (Frotscher, 2010). Indeed, $reelin^{+}$ neurons are still properly located at the surface of the cKO mice and neurons in the upper half are still strongly phospho-cofilin-immunoreactive. Interestingly, however, neurons in the lower part of the cortex, the forming HC, are negative for phospho-cofilin immunolabelling (Figures S6D–S6G) and indeed largely migrate in a tangential manner (Figures 5E–5H). Together, these data prompt the concept that additional signaling mechanisms are sufficient to restrict exceeding G-actin levels in either a WT environment or even the mutant environment in the cortical plate and allow radially oriented migration.

Notably, some of the radially migrating $RhoA^{-/-}$ neurons migrate even further and fail to stop below layer I, forming type II cobblestone lissencephaly after Cre-electroporation and in $Emx1::Cre/RhoA^{fl/fl}$ mice. This neuronal ectopia is also caused by mutations in genes encoding for proteins anchoring BM components (Belvindrah et al., 2007; Costell et al., 1999; Georges-Labouesse et al., 1998; Haubst et al., 2006; Kerjan and Gleeson, 2007; Kleinman and Martin, 2005; Li et al., 2008;

Radakovits et al., 2009; Satz et al., 2010). These anchoring proteins are linked to the actin cytoskeleton via RhoA signaling as is the case for the focal adhesion kinase, a downstream effector of RhoA, and for Galpha12/13 and GPR56 that act upstream of RhoA (Etienne-Manneville and Hall, 2002; Iguchi et al., 2008), which all result in cobblestone lissencephaly when mutated (Beggs et al., 2003; Li et al., 2008; Moers et al., 2008). Thus, RhoA also plays a key role in anchoring BM components, either via the apical dendrite of neurons or via the RG endfeet.

Role of RhoA in RG

In contrast to the surprisingly minor effects of RhoA deletion in neurons, we observed major defects in the RG scaffold as almost the first effect of RhoA deletion. Cortical architecture was disrupted already at the first day when RhoA protein was depleted (E12) due to defects in adherens junction maintenance and defects in RG processes failing to span the entire cortical thickness. Thus, in RG RhoA is not only essential for mediating the apical attachment by adherens junctions (Herzog et al., 2011; Katayama et al., 2011) but also the maintenance or formation of radial processes. Indeed, the actin filament based adhesion belt mediates the strength of adherence also in epithelial sheets (Vasioukhin and Fuchs, 2001). This appears to be similar in the neuroepithelium, where stability cannot be maintained after RhoA depletion resulting in defects in F-actin formation and a converse increase in G-actin. In addition to destabilization of the actin cytoskeleton, we observed the same effect on the microtubular scaffold with a pronounced increase in the dynamic tyrosinated form of MT at the expense of the stabile acetylated tubulin. Notably, this effect on the microtubule stability was much less pronounced in neurons which were still strongly immunoreactive for acetylated tubulin in the absence of RhoA (Figure 7), while no such immunoreactivity was observed in RGs. This is consistent with the requirement of acetylated tubulin for migration and process formation in neurons (Creppe et al., 2009; Heng et al., 2010) and implies cell-type-specific effects of RhoA on the tubulin cytoskeleton in RG. Thus, the effect of RhoA deletion in the developing cerebral cortex causes a profound destabilization of the actin and tubulin cytoskeleton in RG resulting in a loss of apical anchoring and epithelial architecture, as well as defects in basal process formation or maintenance. Together with the results from transplanting WT cells into RhoA cKO cerebral cortices, which also settle either in the upper normotopic cortex or in the SBH, these data demonstrate that defects in RGs are sufficient to cause the phenotype of a double cortex. Thus, even WT neurons after transplantation often do not reach the pial surface and settle in the SBH, while a few of them reach the upper normotopic cortical plate position supposedly when ending up close to a radial glia still in contact with the pial surface. This phenotype obviously worsens during development of the cerebral cortex with more and more radial glial fibers severely disorganized and formation of a progenitor layer separating the upper and lower cortex by E16. Eventually neurons born by progenitors in the lower part of this progenitor layer seem even cut off from signaling pathways, resulting in reduced levels of phospho-cofilin and a predominantly tangential mode of migration as discussed previously and thereby explaining the progressive worsening of the phenotype and the predominant accumulation of late generated neurons in the lower cortex, the SBH.

Double Cortex/SBH As an RG Disorder

These data suggest that "double cortex" formation may result due to defects in RG rather than in the migrating neurons themselves. While the hypothesis that RG defects may contribute to disorders of PH, where misplaced neurons directly appose the ventricle, has been raised (Feng et al., 2006; Sarkisian et al., 2006), this has not been tested and dysfunctions of the RG are not considered to be the sole cause for these malformations. Similarly, the mechanistic basis for SBH, in which the ectopic neurons do not directly appose the ventricle but are embedded into WM structures, has been considered to be a functional defect intrinsic to the migrating neurons themselves (Bielas et al., 2004; Guerrini and Parrini, 2010; Ross and Walsh, 2001).

Interestingly, pathways affected in SBH were largely linked to the MT components of the cytoskeleton, such as Lis1, Dcx, and α-tubulin, with the later requiring acetylation (Creppe et al., 2009; Gleeson et al., 1998; Keays et al., 2007; Reiner et al., 1993), while PH is most often caused by loss-of-function mutations in the Filamin A gene (Guerrini and Parrini, 2010; Robertson, 2004), which crosslinks actin into networks or stress fibers. Moreover, loss of MEKK4 in the mouse resulted in increased phosphorylation of Filamin A and a PH phenotype (Sarkisian et al., 2006), suggesting that Filamin A-mediated regulation of the actin cytoskeleton may be a common pathway in these malformations, even though no such defects were observed after Filamin A deletion (Feng et al., 2006). Interestingly, RhoA depletion affects both the stability of the actin and tubulin cytoskeleton with increased levels in G-actin and tyrosinated tubulin. These alterations result in double cortex formation due to profound defects in RG as clearly demonstrated by electroporation and migration data presented here. Notably, scattering of progenitor cells (and hence RG) is also observed in the TISH rat and HeCo mice, both still unknown mutations, but causing SBH similar to the phenotype observed in the RhoA cKO mice (Croquelois et al., 2009; Fitzgerald et al., 2011; Lee et al., 1997). Heterotopic cortical masses can be also generated by overexpression of wnt ligands due to accumulation of newly generated neurons in the intermediate zone (Munji et al., 2011). Given that scattering of progenitors is not only in the RhoA cKO mice but also in other cases linked to the phenotype of SBH, we propose that defects in the RG scaffold, rather than in migrating neurons themselves, may also account for some other cases of SBH formation caused by mutation of distinct genes.

This view on the etiology of "migrational" disorders has also profound implications for such disorders in human patients as it may help to explain the often rather divergent phenotypes observed in patients and mouse models, as e.g., upon Lis1 or Dcx mutations (Götz, 2003; Kerjan and Gleeson, 2007). Given the profound differences in the RG scaffold in rodent and human cerebral cortex with additional glial cells inserted into the outer SVZ (Fietz et al., 2010; Hansen et al., 2010; Reillo et al., 2010; Smart et al., 2002), which exist only in small numbers in the lissencephalic rodent cerebral cortex (Shitamukai et al., 2011; Wang et al., 2011), a role in RG may well explain these

differences in phenotypes observed in rodents and humans. Indeed, the RG cells in the outer SVZ may be involved in gyrification (Fietz et al., 2010; Reillo et al., 2010), consistent with the concept that defects in their process formation or maintenance may interfere with gyrification and hence result in lissencephalic brains in human patients. Thus, our data prompt a model for lissencephaly and double cortex formation by proposing a key role of the stabilized forms of the tubulin and actin cytoskeleton for RG process maintenance.

EXPERIMENTAL PROCEDURES

Animals

Homozygous *RhoA*$^{fl/fl}$ (Jackson et al., 2011) were crossed to *Emx1::Cre/RhoA*$^{fl/+}$ mice (day of plug = E0) to obtain the *Emx1::Cre/RhoA*$^{fl/fl}$ (cKO) and littermate controls phenotypic WT embryos (*RhoA*$^{fl/fl}$ or *Emx1::Cre/RhoA*$^{fl/+}$). Genotyping was performed by polymerase chain reaction (PCR), and each phenotypic analysis was done with at least three independent litters.

Immunohistochemistry

Immunohistochemistry was performed as described previously (Cappello et al., 2006) with primary antibodies listed in Table S1. Nuclei were visualized by incubating for 10 min with 0.1 μg/ml 4,6-diamidino-2-phenylindole (DAPI; Sigma-Aldrich, St. Louis, MO, USA) in PBS and F-actin filaments by incubation in Texas Red-labeled phalloidin (5 U/ml; Invitrogen, Grand Island, NY, USA). Fluorescent secondary antibodies were used according to the manufacturer's protocol (Jackson ImmunoResearch, West Grove, PA, USA; Southern Biotechnology, Birmingham, AL, USA; Invitrogen), and sections were analyzed using Olympus or Leica laser-scanning microscopes.

In Utero Electroporation

Pregnant mice were operated on as approved by the Government of Upper Bavaria under license number 55.2-1-54-2531-144/07 and were anaesthetized by intraperitoneal injection of saline solution containing Fentanyl (0.05 mg/kg), Midazolam (5 mg/kg), and Medetomidine (0.5 mg/kg;Betäubungsmittel license number: 4518395), and E13/E14 embryos were electroporated as described before (Saito, 2006). pCIG2 containing a GFP or CreGFP, RhoA*GFP and Gap43GFP plasmids were mixed with Fast Green (2.5 mg/μl; Sigma) and injected at the concentration of 1μg/μl. Anesthesia was terminated by Buprenorphine (0.1 mg/kg), Atipamezol (2.5 mg/kg), and Flumazenil (0.5 mg/kg). Embryos were fixed in 4% paraformaldehyde (PFA), and vibratome sections of 100 μm were analyzed using Olympus laser-scanning microscopes.

In Utero Transplantation

Cortical embryonic cells were dissociated and incubated in trypsin for 15 min with green cell tracker (Invitrogen C7025), and 70.000 cells/μl were resuspended in Dulbecco's modified eagle medium, and 1 μl was injected into the ventricle of E13 or E14 embryos. Mice were anaesthetized as described previously. Embryos/pups were fixed in 4% PFA, and vibratome sections of 100 μm were analyzed using Olympus laser-scanning microscopes.

Quantitative Analysis

GFP, Ph3, Tbr1, Ctip2, Cux1, and GAD67$^+$ cells were quantified by counting all positive cells in a radial stripe comprising all cortical layers. Quantifications are given as the mean ± SEM; statistical significance was tested with the unpaired student's t test or unequal variance t test.

c-Fos and Egr-1$^+$ cells were quantified using a NeuroLucida device and StereoInvestigator software (MBF Bioscience, Magdeburg, Germany). Cells were counted in a vertical stripe (layers II–VI). At least five sections for each experimental animal were examined.

Western Blot

Cortices from embryonic brains were lysed in RIPA buffer containing protease and phosphatase inhibitors (Roche, Madison, WI, USA), and 20 μg of total protein were separated by 10% SDS-PAGE and transferred to PVDF membranes (Biorad, Berkley, CA, USA), which were incubated with primary antibodies followed by horseradish peroxidase-labeled secondary antibodies (1:25000; Amersham, Little Chalfont, UK) detected by ECL Western Blotting Detection (Millipore, Billerica, MA, USA). Quantification of bands was performed using ImageJ software. Primary antibodies are listed in Table S1. The G-actin and F-actin fractions were separated by centrifugation (Posern et al., 2002). In order to distinguish between the nuclear and cytoplasmic fraction, we lysed E14 cortical tissue in hypotonic buffer (10 mM HEPES [pH 7.9]). After homogenization, 0.1% NP-40 was added to the lysed samples, and the pellets containing the nuclei were resuspended in hypotonic buffer containing 400 mM NaCl. After sonication and addition of 1% NP40, samples were incubated in ice for 40 min.

DiO Labeling

3,3-dioctadecyboxacarbocyanine perchclorate (DiO) was obtained from Sigma. A crystal of DiO was stuck under the meninges of an intact embryonic brain. Vibratome sections of 100 μm were analyzed using Olympus laser-scanning microscopes.

Live Imaging in Slices

Coronal slices of the embryonic brains were prepared 48 hr after electroporation at a thickness of 300 μm using a vibratome (Leica VT1200S), embedded into collagen matrix (Nitta Gelatin, Cell Matrix type A), subsequently covered with neurobasal medium (GIBCO) with B27 and N2 supplements and 0.45% Glucose and incubated at 37°C in 5% CO_2. Multiple GFP-positive cells were imaged on a confocal microscope (Olympus Fluoview 1000) with a 20× objective. Time-lapse images were captured at intervals of 10 min for 9–12 hr and analyzed using Olympus FV10-ASW1.7 Viewer software and ImageJ.

SUPPLEMENTAL INFORMATION

Supplemental Information includes seven figures, two movies, Supplemental Experimental Procedures, and one table and can be found with this article online at doi:10.1016/j.neuron.2011.12.030.

ACKNOWLEDGMENTS

We would like to thank Stephen Robertson for excellent discussion and comments on the manuscript. We are particularly grateful to Guido Posern, Jeffrey Macklis, Carol Schuurmans, and Michele Studer for antibodies, plasmids, and probes; Gregor Pilz and Sven Falk for help in imaging brain slices; and Detlef Franzen, Timucin Öztürk, Angelika Waiser, Andrea Steiner-Mezzadri, Luise Jennen, Nadin Hagendorf, and Saida Zoubaa for excellent technical help. M.B. has a LMU research fellowship. This work was supported by the Deutsche Forschungsgemeinschaft, including the Leibniz Award and SFB 870, Bundesministerium für Bildung und Forschung, European Union, and the Helmholtz Association.

Accepted: December 14, 2011
Published: March 7, 2012

REFERENCES

Beggs, H.E., Schahin-Reed, D., Zang, K., Goebbels, S., Nave, K.A., Gorski, J., Jones, K.R., Sretavan, D., and Reichardt, L.F. (2003). FAK deficiency in cells contributing to the basal lamina results in cortical abnormalities resembling congenital muscular dystrophies. Neuron *40*, 501–514.

Belvindrah, R., Graus-Porta, D., Goebbels, S., Nave, K.A., and Müller, U. (2007). Beta1 integrins in radial glia but not in migrating neurons are essential for the formation of cell layers in the cerebral cortex. J. Neurosci. *27*, 13854–13865.

Berger, J., Eckert, S., Scardigli, R., Guillemot, F., Gruss, P., and Stoykova, A. (2004). E1-Ngn2/Cre is a new line for regional activation of Cre recombinase in the developing CNS. Genesis *40*, 195–199.

Besson, A., Gurian-West, M., Schmidt, A., Hall, A., and Roberts, J.M. (2004). p27Kip1 modulates cell migration through the regulation of RhoA activation. Genes Dev. *18*, 862–876.

Bielas, S., Higginbotham, H., Koizumi, H., Tanaka, T., and Gleeson, J.G. (2004). Cortical neuronal migration mutants suggest separate but intersecting pathways. Annu. Rev. Cell Dev. Biol. *20*, 593–618.

Bilasy, S.E., Satoh, T., Ueda, S., Wei, P., Kanemura, H., Aiba, A., Terashima, T., and Kataoka, T. (2009). Dorsal telencephalon-specific RA-GEF-1 knockout mice develop heterotopic cortical mass and commissural fiber defect. Eur. J. Neurosci. *29*, 1994–2008.

Cappello, S., Attardo, A., Wu, X., Iwasato, T., Itohara, S., Wilsch-Bräuninger, M., Eilken, H.M., Rieger, M.A., Schroeder, T.T., Huttner, W.B., et al. (2006). The Rho-GTPase cdc42 regulates neural progenitor fate at the apical surface. Nat. Neurosci. *9*, 1099–1107.

Chen, L., Melendez, J., Campbell, K., Kuan, C.Y., and Zheng, Y. (2009). Rac1 deficiency in the forebrain results in neural progenitor reduction and microcephaly. Dev. Biol. *325*, 162–170.

Coleman, J.E., Nahmani, M., Gavornik, J.P., Haslinger, R., Heynen, A.J., Erisir, A., and Bear, M.F. (2010). Rapid structural remodeling of thalamocortical synapses parallels experience-dependent functional plasticity in mouse primary visual cortex. J. Neurosci. *30*, 9670–9682.

Connelly, J.T., Gautrot, J.E., Trappmann, B., Tan, D.W., Donati, G., Huck, W.T., and Watt, F.M. (2010). Actin and serum response factor transduce physical cues from the microenvironment to regulate epidermal stem cell fate decisions. Nat. Cell Biol. *12*, 711–718.

Costell, M., Gustafsson, E., Aszódi, A., Mörgelin, M., Bloch, W., Hunziker, E., Addicks, K., Timpl, R., and Fässler, R. (1999). Perlecan maintains the integrity of cartilage and some basement membranes. J. Cell Biol. *147*, 1109–1122.

Creppe, C., Malinouskaya, L., Volvert, M.L., Gillard, M., Close, P., Malaise, O., Laguesse, S., Cornez, I., Rahmouni, S., Ormenese, S., et al. (2009). Elongator controls the migration and differentiation of cortical neurons through acetylation of alpha-tubulin. Cell *136*, 551–564.

Croquelois, A., Giuliani, F., Savary, C., Kielar, M., Amiot, C., Schenk, F., and Welker, E. (2009). Characterization of the HeCo mutant mouse: a new model of subcortical band heterotopia associated with seizures and behavioral deficits. Cereb. Cortex *19*, 563–575.

Englund, C., Fink, A., Lau, C., Pham, D., Daza, R.A., Bulfone, A., Kowalczyk, T., and Hevner, R.F. (2005). Pax6, Tbr2, and Tbr1 are expressed sequentially by radial glia, intermediate progenitor cells, and postmitotic neurons in developing neocortex. J. Neurosci. *25*, 247–251.

Etienne-Manneville, S., and Hall, A. (2002). Rho GTPases in cell biology. Nature *420*, 629–635.

Feng, Y., Chen, M.H., Moskowitz, I.P., Mendonza, A.M., Vidali, L., Nakamura, F., Kwiatkowski, D.J., and Walsh, C.A. (2006). Filamin A (FLNA) is required for cell-cell contact in vascular development and cardiac morphogenesis. Proc. Natl. Acad. Sci. USA *103*, 19836–19841.

Fietz, S.A., Kelava, I., Vogt, J., Wilsch-Bräuninger, M., Stenzel, D., Fish, J.L., Corbeil, D., Riehn, A., Distler, W., Nitsch, R., and Huttner, W.B. (2010). OSVZ progenitors of human and ferret neocortex are epithelial-like and expand by integrin signaling. Nat. Neurosci. *13*, 690–699.

Fitzgerald, M.P., Covio, M., and Lee, K.S. (2011). Disturbances in the positioning, proliferation and apoptosis of neural progenitors contribute to subcortical band heterotopia formation. Neuroscience *176*, 455–471.

Frotscher, M. (2010). Role for Reelin in stabilizing cortical architecture. Trends Neurosci. *33*, 407–414.

Gandhi, S.P., Yanagawa, Y., and Stryker, M.P. (2008). Delayed plasticity of inhibitory neurons in developing visual cortex. Proc. Natl. Acad. Sci. USA *105*, 16797–16802.

Ge, W., He, F., Kim, K.J., Blanchi, B., Coskun, V., Nguyen, L., Wu, X., Zhao, J., Heng, J.I., Martinowich, K., et al. (2006). Coupling of cell migration with neurogenesis by proneural bHLH factors. Proc. Natl. Acad. Sci. USA *103*, 1319–1324.

Georges-Labouesse, E., Mark, M., Messaddeq, N., and Gansmüller, A. (1998). Essential role of alpha 6 integrins in cortical and retinal lamination. Curr. Biol. *8*, 983–986.

Gleeson, J.G., Allen, K.M., Fox, J.W., Lamperti, E.D., Berkovic, S., Scheffer, I., Cooper, E.C., Dobyns, W.B., Minnerath, S.R., Ross, M.E., and Walsh, C.A. (1998). Doublecortin, a brain-specific gene mutated in human X-linked lissencephaly and double cortex syndrome, encodes a putative signaling protein. Cell *92*, 63–72.

Goebbels, S., Bormuth, I., Bode, U., Hermanson, O., Schwab, M.H., and Nave, K.A. (2006). Genetic targeting of principal neurons in neocortex and hippocampus of NEX-Cre mice. Genesis *44*, 611–621.

Götz, M. (2003). Doublecortin finds its place. Nat. Neurosci. *6*, 1245–1247.

Govek, E.E., Newey, S.E., and Van Aelst, L. (2005). The role of the Rho GTPases in neuronal development. Genes Dev. *19*, 1–49.

Guerrini, R., and Parrini, E. (2010). Neuronal migration disorders. Neurobiol. Dis. *38*, 154–166.

Hall, A., and Lalli, G. (2010). Rho and Ras GTPases in axon growth, guidance, and branching. Cold Spring Harb. Perspect. Biol. *2*, a001818.

Hand, R., Bortone, D., Mattar, P., Nguyen, L., Heng, J.I., Guerrier, S., Boutt, E., Peters, E., Barnes, A.P., Parras, C., et al. (2005). Phosphorylation of Neurogenin2 specifies the migration properties and the dendritic morphology of pyramidal neurons in the neocortex. Neuron *48*, 45–62.

Hansen, D.V., Lui, J.H., Parker, P.R., and Kriegstein, A.R. (2010). Neurogenic radial glia in the outer subventricular zone of human neocortex. Nature *464*, 554–561.

Haubst, N., Georges-Labouesse, E., De Arcangelis, A., Mayer, U., and Götz, M. (2006). Basement membrane attachment is dispensable for radial glial cell fate and for proliferation, but affects positioning of neuronal subtypes. Development *133*, 3245–3254.

Heasman, S.J., and Ridley, A.J. (2008). Mammalian Rho GTPases: new insights into their functions from in vivo studies. Nat. Rev. Mol. Cell Biol. *9*, 690–701.

Heng, J.I., Nguyen, L., Castro, D.S., Zimmer, C., Wildner, H., Armant, O., Skowronska-Krawczyk, D., Bedogni, F., Matter, J.M., Hevner, R., and Guillemot, F. (2008). Neurogenin 2 controls cortical neuron migration through regulation of Rnd2. Nature *455*, 114–118.

Heng, J.I., Chariot, A., and Nguyen, L. (2010). Molecular layers underlying cytoskeletal remodelling during cortical development. Trends Neurosci. *33*, 38–47.

Herzog, D., Loetscher, P., van Hengel, J., Knüsel, S., Brakebusch, C., Taylor, V., Suter, U., and Relvas, J.B. (2011). The small GTPase RhoA is required to maintain spinal cord neuroepithelium organization and the neural stem cell pool. J. Neurosci. *31*, 5120–5130.

Huang, Z.J., Kirkwood, A., Pizzorusso, T., Porciatti, V., Morales, B., Bear, M.F., Maffei, L., and Tonegawa, S. (1999). BDNF regulates the maturation of inhibition and the critical period of plasticity in mouse visual cortex. Cell *98*, 739–755.

Iguchi, T., Sakata, K., Yoshizaki, K., Tago, K., Mizuno, N., and Itoh, H. (2008). Orphan G protein-coupled receptor GPR56 regulates neural progenitor cell migration via a G alpha 12/13 and Rho pathway. J. Biol. Chem. *283*, 14469–14478.

Iwasato, T., Nomura, R., Ando, R., Ikeda, T., Tanaka, M., and Itohara, S. (2004). Dorsal telencephalon-specific expression of Cre recombinase in PAC transgenic mice. Genesis *38*, 130–138.

Jackson, B., Peyrollier, K., Pedersen, E., Basse, A., Karlsson, R., Wang, Z., Lefever, T., Ochsenbein, A., Schmidt, G., Aktories, K., et al. (2011). RhoA is dispensable for skin development, but crucial for contraction and directed migration of keratinocytes. Mol. Biol. Cell *22*, 593–605.

Katayama, K., Melendez, J., Baumann, J.M., Leslie, J.R., Chauhan, B.K., Nemkul, N., Lang, R.A., Kuan, C.Y., Zheng, Y., and Yoshida, Y. (2011). Loss of RhoA in neural progenitor cells causes the disruption of adherens junctions and hyperproliferation. Proc. Natl. Acad. Sci. USA *108*, 7607–7612.

Keays, D.A., Tian, G., Poirier, K., Huang, G.J., Siebold, C., Cleak, J., Oliver, P.L., Fray, M., Harvey, R.J., Molnár, Z., et al. (2007). Mutations in alpha-tubulin cause abnormal neuronal migration in mice and lissencephaly in humans. Cell *128*, 45–57.

Kerjan, G., and Gleeson, J.G. (2007). Genetic mechanisms underlying abnormal neuronal migration in classical lissencephaly. Trends Genet. *23*, 623–630.

Kholmanskikh, S.S., Dobrin, J.S., Wynshaw-Boris, A., Letourneau, P.C., and Ross, M.E. (2003). Disregulated RhoGTPases and actin cytoskeleton contribute to the migration defect in Lis1-deficient neurons. J. Neurosci. *23*, 8673–8681.

Kleinman, H.K., and Martin, G.R. (2005). Matrigel: basement membrane matrix with biological activity. Semin. Cancer Biol. *15*, 378–386.

Kronenberg, G., Gertz, K., Baldinger, T., Kirste, I., Eckart, S., Yildirim, F., Ji, S., Heuser, I., Schröck, H., Hörtnagl, H., et al. (2010). Impact of actin filament stabilization on adult hippocampal and olfactory bulb neurogenesis. J. Neurosci. *30*, 3419–3431.

Lee, K.S., Schottler, F., Collins, J.L., Lanzino, G., Couture, D., Rao, A., Hiramatsu, K., Goto, Y., Hong, S.C., Caner, H., et al. (1997). A genetic animal model of human neocortical heterotopia associated with seizures. J. Neurosci. *17*, 6236–6242.

Leone, D.P., Srinivasan, K., Chen, B., Alcamo, E., and McConnell, S.K. (2008). The determination of projection neuron identity in the developing cerebral cortex. Curr. Opin. Neurobiol. *18*, 28–35.

Leone, D.P., Srinivasan, K., Brakebusch, C., and McConnell, S.K. (2010). The rho GTPase Rac1 is required for proliferation and survival of progenitors in the developing forebrain. Dev. Neurobiol. *70*, 659–678.

Li, S., Jin, Z., Koirala, S., Bu, L., Xu, L., Hynes, R.O., Walsh, C.A., Corfas, G., and Piao, X. (2008). GPR56 regulates pial basement membrane integrity and cortical lamination. J. Neurosci. *28*, 5817–5826.

Lien, W.H., Klezovitch, O., Fernandez, T.E., Delrow, J., and Vasioukhin, V. (2006). alphaE-catenin controls cerebral cortical size by regulating the hedgehog signaling pathway. Science *311*, 1609–1612.

Lodato, S., Rouaux, C., Quast, K.B., Jantrachotechatchawan, C., Studer, M., Hensch, T.K., and Arlotta, P. (2011). Excitatory projection neuron subtypes control the distribution of local inhibitory interneurons in the cerebral cortex. Neuron *69*, 763–779.

Machon, O., van den Bout, C.J., Backman, M., Kemler, R., and Krauss, S. (2003). Role of beta-catenin in the developing cortical and hippocampal neuroepithelium. Neuroscience *122*, 129–143.

Malatesta, P., Hartfuss, E., and Götz, M. (2000). Isolation of radial glial cells by fluorescent-activated cell sorting reveals a neuronal lineage. Development *127*, 5253–5263.

Moers, A., Nürnberg, A., Goebbels, S., Wettschureck, N., and Offermanns, S. (2008). Galpha12/Galpha13 deficiency causes localized overmigration of neurons in the developing cerebral and cerebellar cortices. Mol. Cell. Biol. *28*, 1480–1488.

Molyneaux, B.J., Arlotta, P., Menezes, J.R., and Macklis, J.D. (2007). Neuronal subtype specification in the cerebral cortex. Nat. Rev. Neurosci. *8*, 427–437.

Munji, R.N., Choe, Y., Li, G., Siegenthaler, J.A., and Pleasure, S.J. (2011). Wnt signaling regulates neuronal differentiation of cortical intermediate progenitors. J. Neurosci. *31*, 1676–1687.

Nguyen, L., Besson, A., Heng, J.I., Schuurmans, C., Teboul, L., Parras, C., Philpott, A., Roberts, J.M., and Guillemot, F. (2006). p27kip1 independently promotes neuronal differentiation and migration in the cerebral cortex. Genes Dev. *20*, 1511–1524.

Pacary, E., Heng, J., Azzarelli, R., Riou, P., Castro, D., Lebel-Potter, M., Parras, C., Bell, D.M., Ridley, A.J., Parsons, M., and Guillemot, F. (2011). Proneural transcription factors regulate different steps of cortical neuron migration through Rnd-mediated inhibition of RhoA signaling. Neuron *69*, 1069–1084.

Pinheiro, E.M., Xie, Z., Norovich, A.L., Vidaki, M., Tsai, L.H., and Gertler, F.B. (2011). Lpd depletion reveals that SRF specifies radial versus tangential migration of pyramidal neurons. Nat. Cell Biol. *13*, 989–995.

Posern, G., Sotiropoulos, A., and Treisman, R. (2002). Mutant actins demonstrate a role for unpolymerized actin in control of transcription by serum response factor. Mol. Biol. Cell *13*, 4167–4178.

Radakovits, R., Barros, C.S., Belvindrah, R., Patton, B., and Müller, U. (2009). Regulation of radial glial survival by signals from the meninges. J. Neurosci. *29*, 7694–7705.

Reillo, I., de Juan Romero, C., Garcia-Cabezas, M.A., and Borrell, V. (2010). A role for intermediate radial glia in the tangential expansion of the mammalian cerebral cortex. Cereb Cortex. 10.1093/cercor/bhq238.

Reiner, O., Carrozzo, R., Shen, Y., Wehnert, M., Faustinella, F., Dobyns, W.B., Caskey, C.T., and Ledbetter, D.H. (1993). Isolation of a Miller-Dieker lissencephaly gene containing G protein beta-subunit-like repeats. Nature *364*, 717–721.

Robertson, S.P. (2004). Molecular pathology of filamin A: diverse phenotypes, many functions. Clin. Dysmorphol. *13*, 123–131.

Ross, M.E., and Walsh, C.A. (2001). Human brain malformations and their lessons for neuronal migration. Annu. Rev. Neurosci. *24*, 1041–1070.

Saito, T. (2006). In vivo electroporation in the embryonic mouse central nervous system. Nat. Protoc. *1*, 1552–1558.

Sarkisian, M.R., Bartley, C.M., Chi, H., Nakamura, F., Hashimoto-Torii, K., Torii, M., Flavell, R.A., and Rakic, P. (2006). MEKK4 signaling regulates filamin expression and neuronal migration. Neuron *52*, 789–801.

Satz, J.S., Ostendorf, A.P., Hou, S., Turner, A., Kusano, H., Lee, J.C., Turk, R., Nguyen, H., Ross-Barta, S.E., Westra, S., et al. (2010). Distinct functions of glial and neuronal dystroglycan in the developing and adult mouse brain. J. Neurosci. *30*, 14560–14572.

Shitamukai, A., Konno, D., and Matsuzaki, F. (2011). Oblique radial glial divisions in the developing mouse neocortex induce self-renewing progenitors outside the germinal zone that resemble primate outer subventricular zone progenitors. J. Neurosci. *31*, 3683–3695.

Smart, I.H., Dehay, C., Giroud, P., Berland, M., and Kennedy, H. (2002). Unique morphological features of the proliferative zones and postmitotic compartments of the neural epithelium giving rise to striate and extrastriate cortex in the monkey. Cereb. Cortex *12*, 37–53.

Vartiainen, M.K., Guettler, S., Larijani, B., and Treisman, R. (2007). Nuclear actin regulates dynamic subcellular localization and activity of the SRF cofactor MAL. Science *316*, 1749–1752.

Vasioukhin, V., and Fuchs, E. (2001). Actin dynamics and cell-cell adhesion in epithelia. Curr. Opin. Cell Biol. *13*, 76–84.

Wang, X., Tsai, J.W., LaMonica, B., and Kriegstein, A.R. (2011). A new subtype of progenitor cell in the mouse embryonic neocortex. Nat. Neurosci. *14*, 555–561.

Wheeler, A.P., and Ridley, A.J. (2004). Why three Rho proteins? RhoA, RhoB, RhoC, and cell motility. Exp. Cell Res. *301*, 43–49.